

Article

Possible Geometries for Precast Concrete Structures, through Discussing New Connections, Robotic Manufacturing and Re-Utilisation of the Concrete Elements

Abtin Baghdadi , Lukas Ledderose * and Harald Kloft 

Institut für Tragwerksentwurf (ITE), Technische Universität Braunschweig, 38106 Braunschweig, Germany; a.baghdadi@tu-braunschweig.de (A.B.)

* Correspondence: l.ledderose@tu-braunschweig.de

Abstract: This study explores the potential use of new connections to shape precast building geometries, focusing on connection performance, robotic fabrication, and foldable structural elements. Three connection types, including coupled-bolts, hinges, and steel tubes, were initially proposed and assessed in beam and portal frame geometries. In contrast, the study introduces conceptual ideas; initial experimental and numerical studies were conducted to estimate connection capacities. Robotic fabrication for connecting elements to reused concrete and converting floor elements into beams was detailed, showcasing robotic technology's performance and potential. These connections were employed in designing new precast element geometries, ranging from simple beams to multi-story buildings. Geometric properties and volume quantities of folded and opened geometries were studied using 37 CAD models. To properly discuss the joint performance reference, monolithic elements with exact dimensions were created for comparison. Despite varied connection capacity (38% to 100%), the steel tube exhibited the most desirable performance, resembling a monolithic element with an exact size. Some proposed foldable geometries showed a significant reduction (up to 7%) in element dimensions to facilitate transport and construction.

Keywords: foldable; geometries; precast; hinges; connections; experimental; numerical



Citation: Baghdadi, A.; Ledderose, L.; Kloft, H. Possible Geometries for Precast Concrete Structures, through Discussing New Connections, Robotic Manufacturing and Re-Utilisation of the Concrete Elements. *Buildings* **2024**, *14*, 302. <https://doi.org/10.3390/buildings14010302>

Received: 15 December 2023

Revised: 11 January 2024

Accepted: 15 January 2024

Published: 22 January 2024



Copyright: © 2024 by the authors. Licensee MDPI, Basel, Switzerland. This article is an open access article distributed under the terms and conditions of the Creative Commons Attribution (CC BY) license (<https://creativecommons.org/licenses/by/4.0/>).

1. Introduction

The construction sector and cement manufacturing consume substantial quantities of natural resources. Yet, extracting the natural aggregates required to manufacture concrete and mortars is becoming increasingly difficult due to quarry depletion, environmental impact, and regulations. Thus, the search for solutions is an urgent matter. Prefabrication could be a potential answer. Prefabricated elements have gained popularity in the construction industry, particularly in nations such as Canada and Japan. In European countries such as Germany and the Netherlands, precast construction accounts for more than 35% of the building sector [1]. International strategies are being established to improve sustainability, encouraging precast companies to further increase sustainability through their operations. One such policy is the British Precast Concrete Federation's "Precast Sustainability Strategy and Charter", which became mandatory in Britain in 2014. In addition, EU regulations require compliance with the "Sustainable Use of Natural Resources" criterion [2], which mandates that construction projects are conceived, constructed, and demolished in a manner that preserves natural resources [3].

Prefabricated concrete structures are becoming increasingly common in the architectural, engineering, and construction industry (AEC). This process entails constructing a building with factory-produced precast concrete components assembled on-site [4]. Compared to typical on-site casting methods, this strategy involves fewer on-site operations and labour resources, resulting in improved construction quality, shorter construction duration, and less environmental contamination [5,6]. However, producing prefabricated concrete

structures is complicated and requires multiple operations, including component shipping, storage, and installation [2,7]. These are crucial procedures, especially in projects in urban areas with limited space [8]. Failure to organise these operations correctly can result in problems such as storage difficulties and lead to significant construction delays [7,9]. The high use of natural resources in the precast industry prompted researchers to investigate the feasibility of re-utilising demolished structures' components in new precast constructions.

Reutilisation: The demolition and replacement of old and dilapidated buildings and traffic infrastructure is common practice in many parts of the world today. This is often the result of changes in usage, decay, urban reorganisation, and natural disasters. Around 850 million tonnes of construction and demolition waste are generated annually in the European Union, representing 31% of all global construction-related waste [10]. In the United States, an estimated 123 million tons of construction waste are produced from demolition activities each year [11].

Handling building and demolition waste has been a concern for decades, with landfill disposal being the most common solution. Yet, this process generates enormous waste deposits, leading to environmental contamination. Meanwhile, the demand for concrete continues to rise, resulting in increased consumption of natural aggregate as the principal component of concrete. The concrete industry is the world's largest consumer of natural resources [12], consuming a staggering 12.6 billion tons of raw materials annually. Over two and a half billion tons of aggregate are produced annually in the United States alone, and this number is projected to rise [11]. In response, some European nations have taxed virgin aggregates to encourage their protection. Sustainable construction is no longer merely an ideal but a fundamental necessity. Investigating means of minimising the industry's environmental impact and promoting the recycling of building and demolition waste [10].

Recycling this debris for new construction projects has economic and environmental benefits and is gaining increasing global attention. However, the feasibility of reusing concrete greatly depends on the project's location [13]. Due to the limited availability of resources in a particular region, surrounding concrete structures may be removed and reused as a roadway base or coarse aggregate for concrete. The usage of recycled concrete as a granular basis is rising quickly, as evidenced by the recycling of 145,000 tons of concrete from old terminals and pavements at Toronto Pearson Airport for use as granular base layers [13]. Reusing elements from demolished concrete structures in new construction has been practised for decades, although it presents various obstacles. Changes in the material, such as corrosion in steel, pose one of the greatest obstacles but can be mitigated by various methods. Another challenge is the attachment of connections to the elements, as there often is a lack of connection types and attachment techniques designed for re-utilisation. Hence, in addition to establishing new connections, automated processes are required to address these issues, [14,15].

Robotic Manufacturing: Prefabrication is widely recognised as an efficient and effective alternative to conventional construction techniques. This strategy offers numerous benefits, including reduced material usage, increased safety, increased labour efficiency, improved craftsmanship, uninterrupted workflow, and lower project duration, costs, and waste [16–18]. Despite these benefits, the industry faces multiple difficulties such as complex interfacing between components, [18] reliance on conventional methods [19], cost barriers [16], underutilisation of manufacturing facilities, scheduling difficulties, fragmented information, and quality inconsistencies [20,21]. Previous research has studied and demonstrated the potential for advanced manufacturing and robotic technologies to overcome these constraints and exploit the advantages of prefabrication [22]. In recent years, the use of robotic technology in the prefabrication process has made significant technological advances, enabling or streamlining numerous manufacturing activities.

An analysis of the application of automated and robotic systems in controlled off-site conditions for various building materials [22] determined that these technologies play a crucial role in delivering high-quality and accurate results while enhancing productivity and safety [23]. Despite the benefits of robotics in building prefabrication, it is still not

widely used. To reach the full potential of robotics in building prefabrication, it is necessary to better comprehend its adoption and implementation [24]. In addition, academics have investigated the adoption of many information technologies in the construction industry [25,26]. The attachment of joints to the prefabricated or repurposed pieces is one of the difficulties that robotic production can mitigate. Therefore, it is necessary to design and study suitable joining mechanisms. One of the types of joints that can be produced by robotic manufacturing is dry concrete joints. Essentially, to avoid complicated and uneconomical joint applications, the robotic CNC method was employed to create dry concrete joints with high interlocking and robustness [27].

FE and Experimental analysis: According to earlier studies [28,29], the performance of these joints under various types of loads has been examined using both finite element calculations [30] and experimental tests [31]. The purpose of these studies was to analyse the performance of the joints, identify their principal failure mode, as well as determine joint dimensions and specifics. These studies demonstrated the accuracy of the finite element method for designing and evaluating joints. Specifically, it was demonstrated that numerical modelling can assess the mechanical behaviour of joints [32].

Several studies have utilised Abaqus to analyse the stresses in joints and understand their unique characteristics [33,34]. Due to the complex calculations and evaluation of the geometries, the Displacement-Based design approach [35] is frequently employed by researchers. The results of these studies indicate that such joints can retain between 70–92% of the beam's rigidity and 55–57% of its total bearing capacity [36]. The full-scale experiments [35] and (1/3)-scale experimental studies of connections [37] published provide valuable insights into the 'real' behaviour of such linkages. Aside from the joint geometry and material, the post-tensioning technique is another essential factor for these precast applications. The proper application of non-adherent post-tensioning techniques could significantly increase the performance of the connections [38] and address some of the typical challenges of precast systems stated above, such as transportation and storage.

Foldable elements: Modern approaches to the responsiveness of architectural components tend to eliminate moving parts as much as possible, minimising the use of complex mechanisms [39]. This primarily simplifies their management by reducing the need for frequent maintenance operations. Such procedures are frequently neglected due to negligence or high costs, resulting in the premature degradation of component performance. An alternate solution is elastic kinematics [40]. Foldable components may form an entire building, including its structure, particularly in small buildings or temporary pavilions [41] or merely involve specific building components [42].

Origami-based systems are one of the well-developed techniques using foldable elements [40,43]. They can exhibit unique properties such as tunable stiffness [44], tunable chirality [45], tunable thermal expansion [46], programmable collapse [47], multi-stability [44,48], and self-foldability, making them promising candidates for applications such as re-configurable architect-ed materials. Despite these potentials of origami-based design approaches demonstrated by recent advances in the field [48,49], the lack of robust, application-driven design standards and scalable manufacturing processes has limited their uses [50,51].

Additionally, in the following steps, other types of already developed structural approaches can find their places in new assembly and designing strategies for re-utilising the structural elements, such as approaches for finding optimum places for locating the connections [52] or allocating optimum locations to the elements in the newly designed structures [53].

This paper intends to investigate unique precast geometries and assess the possibilities of robotic subtractive production to highlight the precast industry's relevance, the necessity for investigating new geometries, and the significance of concrete reuse. In order to successfully demonstrate the proposed concepts, semi-novel joints will be tested and numerically evaluated for their application in robotic manufacturing. Several geometries

for precast components and structures will be presented and discussed using the examined connections to simplify transportation, storage, and construction.

2. Discussions

This article's primary aim is to propose and assess the feasibility of utilising new structural forms to develop foldable structures. The study also delves into the practical implementation of robotic techniques and the reuse of old elements. Hence, the article's main body is divided into three sections: a discussion of the connection types, examples of robotic attachment techniques for the joints, and a proposal for precast geometries. The experimental and numerical methods were chosen to evaluate the performance of five connections based on their capacities, force-deformation diagrams, and stresses. These geometries serve as the base for the following sections.

The second section focuses on re-utilising concrete components and robotic manufacturing processes. A flooring slab was selected as the "old element" and processed into beams, studying the robotic attachment of the three types of connections by an automated subtractive process (sawing, milling, and drilling). The last part illustrates 37 potential geometries for precast concrete elements, in which the previously discussed connections were used, and geometrical peculiarities in comparison between the transporting geometries and final form were discussed. In addition, the differences between their transport geometries (folded structures) and the final form (erected on site) are discussed.

- Evaluation of the connections
- Robotic connection attachment to re-utilised elements
- Geometries for concrete precast structures

2.1. Evaluation of the Connections (C_{1-5})

2.1.1. Methodology

Evaluation of joint performance by four-point bending tests is a common method in which the joint is tested for its pure bending moment. This technique evaluated the beam (head-to-head) and the connections (C1, C2, and C4). All experiments were subject to identical test setups (Figure 1). The hinge and the steel tube for the head-side (beam-support) detail were evaluated in frames, and the connections were evaluated under simultaneous bending moments and shear forces (C3 and C5). All elements, including the elements in fold-able geometries, in this study, have a cross-section of 10×10 cm; the length of the beams used in both experimental setups is 1 m, and the height of the frame columns is 50 cm, Figure 2. Formwork with beam and frame shapes was made to prepare the models, and the material's properties were tested. To prepare the specimens, beam and frame-shaped formwork was created, and the material's properties were evaluated. In the four-point bending test of the beams, the separation between the two test loads generated by the hydraulic pump was maintained at 24 cm, surpassing the length of the connections. Furthermore, the spacing between the supports measured 24×3 cm. In the portal frame, the bottom sides of the columns had fixed supports, while the length of the beam was 1 m, and the height of the side columns was 0.5 m. Figure 1 illustrates a tested portal frame. Forces were measured at the middle of the top beam; additionally, a photograph of the formwork with the L-tube showcasing a setup. Similar setups were used for the beam; however, for the beam, supports were positioned directly beneath the beams.

After initial calculations and technical evaluations, similar main reinforcing bars were designed for all beams (No. 4, $\phi 10$). In addition to the standard calculation of the section capacity, a monolithic beam and a monolithic frame made of the same material were tested in the same setup and compared. Based on the ACI (standard) and Section Designer from SAP2000, the ultimate capacity of a cross-section (10×10 cm) with tension bars only ($2\phi 10$ mm) is 6.2 kN.m, and with compression bars and applied prestressing forces, it is 7.9 kN.m. The specimens also use shear reinforcement ($\phi 6$ mm = @ 12.5 cm). Concerning the concrete properties (f_c : 45 MPa) and the selected stirrups, the standard shear force capacity

($V_u = 0.75(V_c + V_s)$) is 18 kN. The safety factor of the standards was also considered in the comparisons.

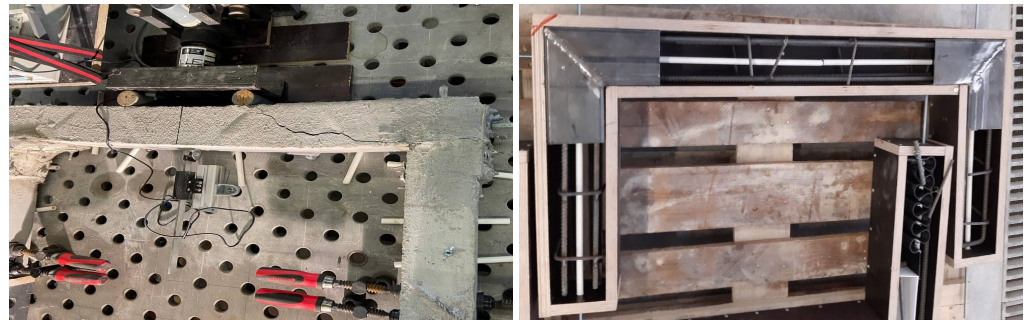


Figure 1. The testing setup and form-work of two portal frames' connections (C₃ and C₅).

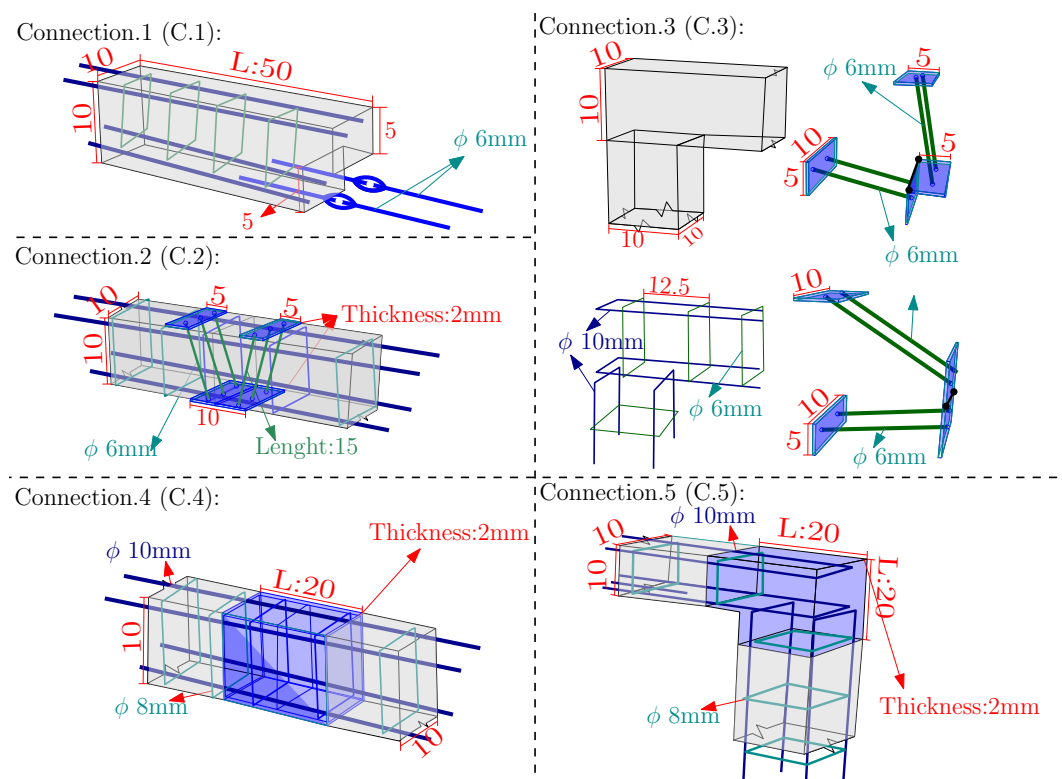


Figure 2. Demotions and parameters of the connections (C₁₋₅), unit (cm).

Abaqus (2019) was used in the finite element analysis, and the material properties were calculated and assigned based on catalogues, tests, and references. Concrete damage plasticity was selected in the property module of Abaqus. Based on [54,55], a bi-linear approach was calculated for tensile behaviour, while compressive behaviour is defined according to codes [56]. The yield parameters for plasticity are defined according to [54,55]. The interaction module, hard contact by mechanical tangential behaviour, was selected to define the contact properties. In addition, the method of normal behaviour and linear friction (Penalty 0.3) was applied [57,58]. Regarding the catalogue, the steel properties (B500B) were assigned in Abaqus. During the tests, the load was incrementally increased up to the complete failure of the segment. A similar performance was simulated in FE analyses, and the verified performances were discussed for each connection compared to the monolithic reference.

2.1.2. Connection 1

Generally, beams are elements performing under tension (e.g., on the bottom side) and compression (e.g., on the top side) of the section, forming a couple in a section between the compression concrete and tensile longitudinal rebars. Preparing a robust connection between the tensile elements and activating the rebars is the primary challenge in these connections. Additionally, modern production techniques require novel structural approaches. One such concept could be using a connector or coupling between the discontinued rebars to transmit the tensile loads. In this proposed joint (C_1), as shown in Figure 3, the idea was evaluated, in which two screws (or rebar) protruded on the underside of each part from the specimen end to the cut-out portion in preparation to connect the four elements two by two. Oval-shaped connectors easily connect these outgoing screws. The oval-shaped connectors, which are readily available on the market, have nuts at their ends, and by rotating the oval connector (Figure 3), the prepared screws can easily find their place, allowing for a continuous longitudinal connection between the tensile rebars. Adding screw-shaped profiles to the rebar or adding extra long screws and using a different coupling as is used in the current experiment is possible. In the case of using extra elements, referring to the standard can assist in calculating the overlap between the screw and rebar when using extra elements.



Figure 3. C_1 , rebar layout and geometrical dimensions.

C_1 has robust behaviour performing at 54% of the monolithic beam's bending capacity, which was 3.74 kN.m. Additionally, the capacity ratio in 10 mm of deformation was raised to 68%. This capacity can also be achieved by increasing the length and dimensions of the rebar or by adding plates to the ends of the screws. Although in this study, the screws (ϕ 6 mm) were located a little higher than the rebar (ϕ 10 mm), which reduces the capacity of this technique, the performance of the proposed connection was comparable to that of a monolithic beam. The failure crack occurred on the underside of the specimens due to screw movement and the resulting damage to the concrete in this area. Based on the confirmed simulation results, this geometry can activate the rebars (screws). The amount of steel stress in the first crack moment increased up to 38% of the allowed amount, while in the compressed concrete, over 80% of the allowed concrete stresses were reached.

Cutting or milling can quickly produce this voided part of the elements. The robotic technique can also drill holes (for locating rebar or screws) and apply glue if necessary. Because the deformation is primarily based on the elongation of the steel rebar, the "force-deformation diagram" gradually curves without a sudden failure (Figure 4).

2.1.3. Connection 2

As mentioned briefly above in Section 2.1.2, adding simple accessories (e.g., steel hinges) and elements to the concrete parts and connections should be studied to potentially develop a new construction approach or a new school of thought. One idea that may be a small part of this new school of thought is attaching steel hinges between two precast structural elements, e.g., beam-beam, column-column, or floor-floor connections. These steel hinges perform predominantly under just one type and direction of loads, e.g., tension. This idea enables the engineer to use the folded frame or floors. For instance, as a new construction approach, the precast frames can be connected during manufacturing to simplify transportation in the construction process. After being transported as paralleled elements, their final form can be opened up in a suitable direction to perform as a portal frame or multi-floor slab.

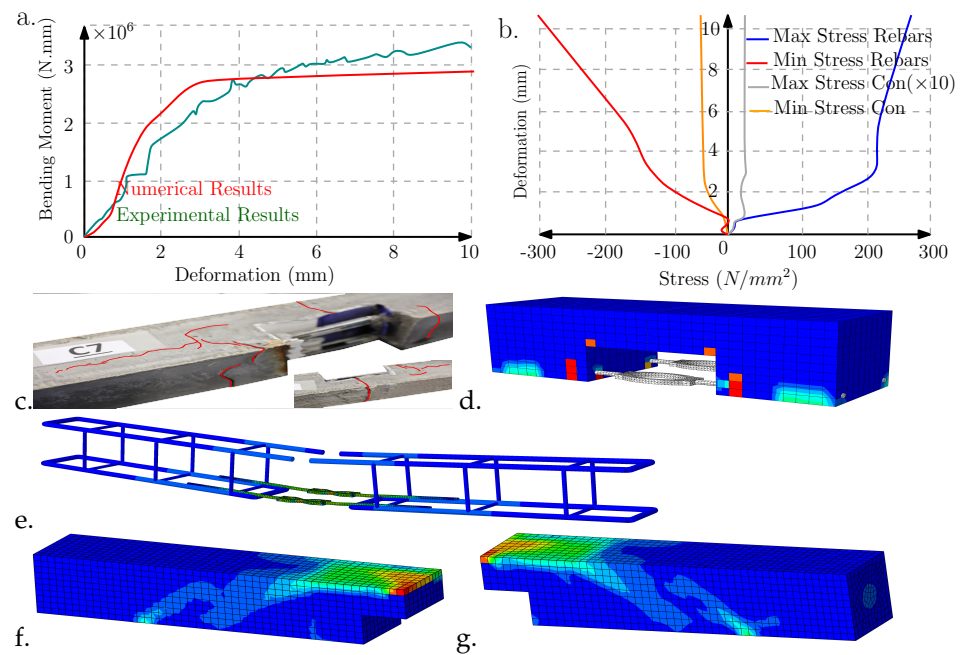


Figure 4. C1, (a) Experimental and numerical bending-deformation, (b) numerical tensile and compressive stress in the steel and concrete, (c) experimental cracks, (d) numerical cracks, (e) principal stress of rebars, (f,g) concrete Von Mises stress.

Inspired by the mentioned idea, the current experiment uses a hinge as an element's tensile component and the concrete's top side as the compressive couple in the section. The tested connection was made by one inexpensive hinge from the hardware store ($10 \times (5 + 5)$ cm). Typically, the hinges have three different screw holes on each side. These three holes (each 3×2) were connected to same-sized plates on the opposite side of the same specimen by three 4 mm screws Figure 5. This technique sends the forces to the top side of the beam's section. The experienced bending capacity of this joint was $1.9 \times$ kN.m which is 27% of the capacity of the entire section and increases to 38% in 10 mm deformation.

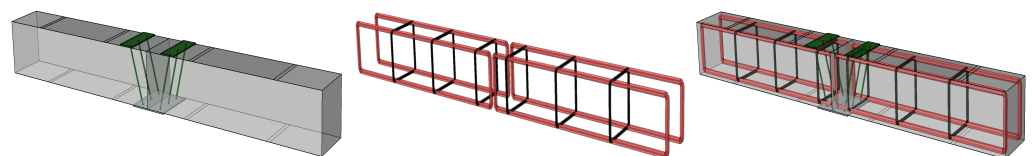


Figure 5. C2, rebar layout and geometrical dimensions.

The capacity was limited due to the selection of low-quality products on the market, including the screws and hinges. The concrete surface resisted the connection to surface compression and the post-tensioning load. Then, in another step, once the hinge was activated, the couple between the compressive concrete and tensile hinge started. Regarding the experienced result, the failure mainly comes from the movement and/or damage of the screws for connecting the top and bottom plates, especially in connecting to the bottom plate and separating the hinges' rings, due to the quality of the hinges, Figure 6. This means using more robust hinges can quickly and considerably increase the capacity of this type of connection. The needed place for using screws, plates, etc., can be easily machined by robotic CNC.

2.1.4. Connection 3

Likewise, the main aim of this geometry is to use foldable elements for the sweep construction of precast concrete structures. Aside from limited details for making concrete

hinges in monolithic elements (e.g., crossing of all rebars of the element in one point of the section), none can be used practically in beam and column precast systems to fold the elements with robust performance. Therefore, this section proposes a geometry using hinged-steel performance for connecting concrete elements, with no dry concrete connection to be experimentally and numerically evaluated, Figure 7.

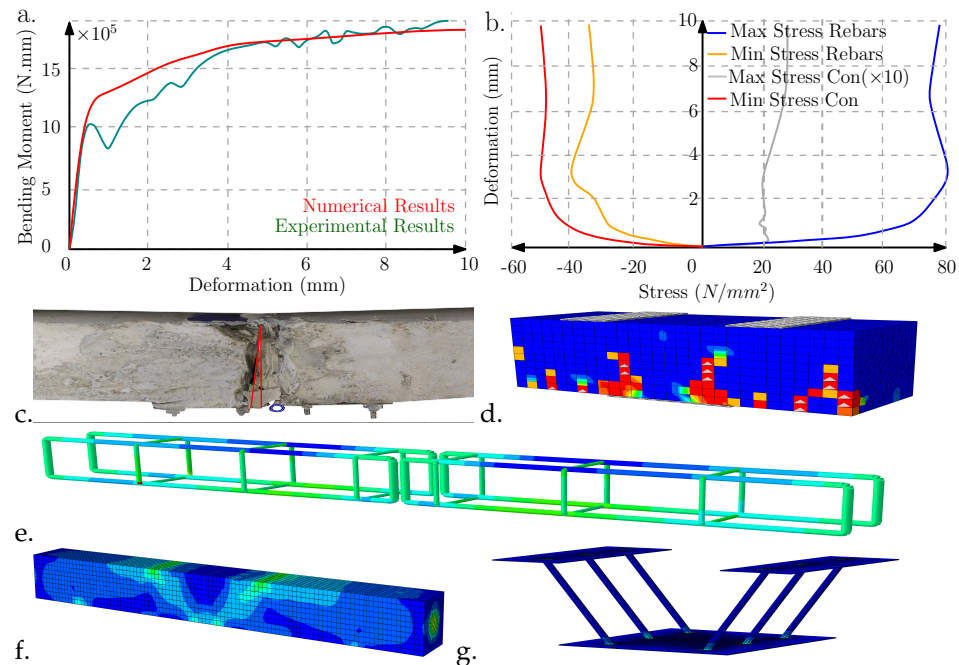


Figure 6. C2, (a) Experimental and numerical bending-deformation, (b) numerical tensile and compressive stress in the steel and concrete, (c) experimental cracks, (d) numerical cracks, (e) principal stress of rebars, (f,g) concrete and hinge Von Mises stress.

Similar to Connection 2, the inexpensive hinges were located on the outer side on one side of the frame and the inner side on the other side of the frame (α), Figure 8. The hinge plates were perpendicular to each plate (β), causing a non-symmetrical geometry Figure 7. The selected hinges typically have two plates, each 2 mm thick and with three holes. The holes above the hinge plates are connected to the concrete sections with some screws (radius: 4 mm). They cross the sections up to the other side, where the three longitudinal screws are connected to the second single palate. This connected frame's measured force was increased to 44.26 kN, resulting in 22.134 kN and 3.9 kN.m shear and bending loads, respectively. In this geometry, the performance of the hinges has the greatest influence on the capacity of the geometry. According to the numerical results, the highest stress occurred between the hinges, the hinge plates, and the screws. Correspondingly, the failure occurred due to the failure of the hinges, which separated the knuckles of the hinges that enclose the pins. On the left side of the top beam, where the hinge was located on the underside of the frame, shear-bending cracks were experienced, which were the main collapsing reason for this geometry similar to the reference frame. It shows the stiffness of the connections with the hinges on the outer side (α) is higher, leading to greater force absorption.

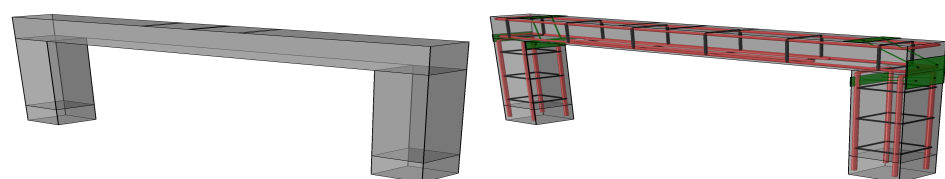


Figure 7. C3, rebar layout and geometrical dimensions.

The robotic CNC of this system can be managed by drilling techniques, which can easily create parallel holes through the section width at exact angles. The angle of the screws in the section influences the connection capacity that interacts with the essential dimension of the screw and nuts for achieving the necessary cohesiveness with the concrete to stop screw movement and rupture the angles and loads, additionally causing the elements to be pushed to each other.

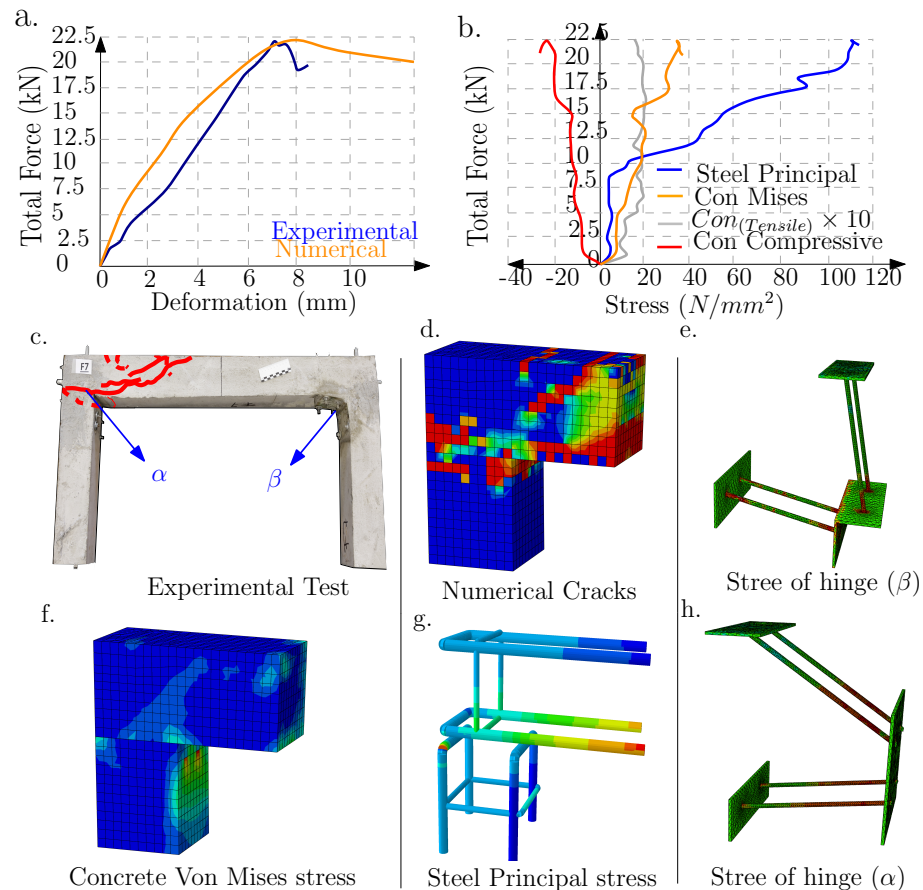


Figure 8. C3, (a) Experimental and numerical force-deformation, (b) numerical tensile and compressive stress in the steel and concrete, (c) experimental cracks, (d) numerical cracks, (e) principal stress of hinges, (f) Von Mises stress in concrete, (g,h) principle stress in rebar and hinge.

2.1.5. Connection 4

The purpose of this proposed geometry (C_4) is to compare the performance of dry concrete joints to that of the steel tube connections. As the most robust proposed connection, instead of a dry concrete connection, C_4 benefits from one steel tube with a rectangular section. The length of the steel tube is 200 mm, and the thickness of all four faces is 2 mm. In addition to simple robotic or manual production, this joint resisted up to 69% of the monolithic section's bending capacity. This ratio increased to 86% in 10 mm deformation. The high shear and torsion capacities are predictable since all connecting zones surround the steel tube (Figure 9).



Figure 9. C4, rebar layout and geometrical dimensions.

Another important point about this simple geometry is that it is easily adjustable. For instance, by increasing the length and thickness of the tube, the bending capacity can easily be increased, exceeding the concrete section's capacity. This joint's capacity can easily be calculated based on various steel standards. And finally, as shown by the final geometries, C_4 can be practically used for various types of connections, e.g., column–column or beam–column. The general performance was similar to the reference beam. However, the failure mainly occurred due to concrete compression collapses caused by hard contact with the opposing side and the steel tube while moving out from the steel tube. The post-tensioning load had initially prevented this. In 2.2 mm deformation, the compressive concrete and tensile rebar stress ratios were 100% and 27%, respectively. The experiment showed that both concrete specimens and initial cracks somehow moved out of the tube when the compressive stress ratio in the rebar was raised to 57%. Deformation of the tube to an inflated shape on the downer side occurred (Figure 10), which can be improved by increasing the post-tensioning forces. The performance of the L-shape connections differs from other joints. In this geometry, the primary resistance is solely from the steel tube, unlike in other joints where the highest stresses may vary and move across different steel parts and zones. This variation led to a robust single-step failure, resulting in the element's collapse. This dynamic performance is evident in the top end of the diagrams.

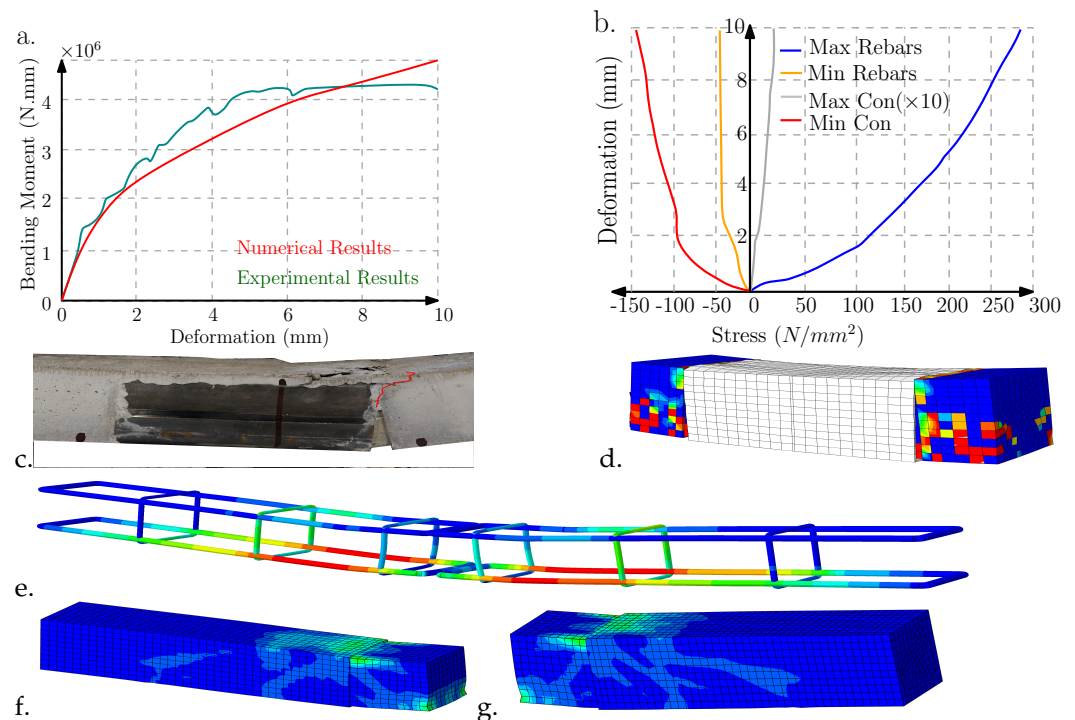


Figure 10. C_4 , (a) experimental and numerical bending-deformation, (b) numerical tensile and compressive stress in the steel and concrete, (c) experimental cracks, (d) numerical cracks, (e) principal stress of rebar, (f,g) Von Mises stress in concrete.

For more robust performance and increased thickness, one plate perpendicular to the sides of the tube was located in the middle. Although this plate (2 mm thick) improves the structural performance of this connection by preventing an increase in the local buckling factor, its primary function is to prevent the unintended movement of the elements within the tube, which should be considered in a building structure. Generally, utilising steel in different structural elements, if no screw failure or welding rupture occurs, causes gradual deformation without sudden loss of stiffness. This experiment had no sudden collapse, even after 20 mm of deformation. The force amount was also slightly increasing, see Figure 10.

2.1.6. Connection 5

Figure 11, displays that, similar to Connection 4, this frame uses an L-shaped steel connection with a tube-box-shaped section (2.5 mm thick). It should be considered that the robotic CNC technique can also create suitable geometries from the printed concrete surfaces for attaching steel elements to the concrete, e.g., for steel tubes and adding screws. This experimental and numerical analysis showed that this connection performs more robustly than the monolithic reference frame. The testing force for evaluation of this geometry applied a $5.15 \text{ kN} \cdot \text{m}$ bending load and a 30.815 kN shear force.

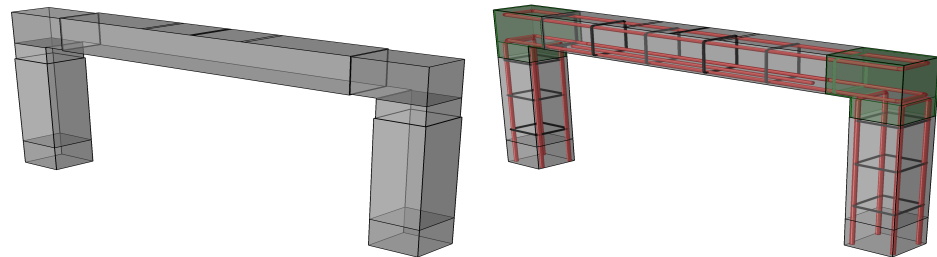


Figure 11. C5, rebar layout and geometrical dimensions.

The failure occurred outside the steel boxes when the top beam approached its shear capacity in a lower bending position. It indicates that the connection was more robust than the frame, and the failure part moved slightly out of the box. This robustness increased the stiffness of this geometry up to $141.1 \text{ N} \cdot \text{M}/\text{tag}(\theta)$, which is 1.45 times higher than the monolithic frame. At the moment of failure, when the concrete reached its maximum compressive capacity, the steel stresses of the longitudinal rebar in the top-mid beam rose to 24% of the allowed stress, Figure 12. Utilisation of such detail and robust performance has different advantages, such as being calculatable based on steel standards and since each geometry has some geometrical parameters, which make it possible to adjust the geometries of the connections (e.g., concrete dry connections [33,59] and their capacities). The geometric parameters are generally interrelated, and increasing one parameter can lead to a reduction in another. However, parameters, including the length, thickness, or additional stiffeners, can be freely selected in such a steel geometry. Furthermore, CNC operations of this geometry over the printed material are reasonable, both financially and time-wise.

2.2. Robotic Subtractive Operation for Connection Attachment to Re-Utilised Elements

Reusing concrete elements and leveraging robotic manufacturing capabilities are current topics in various studies. Concrete, the second most consumed material globally, generates 4.4 billion tons annually, prompting the need to address carbon dioxide emissions. Reusing old elements poses challenges such as proper cutting during demolition, material quality evaluation, adherence to current standards, and assembly in new structures. This highlights the importance of finding new adaptable purposes for their use. Determining the feasibility of repurposing elements, like using a column as a beam or reusing floor elements, requires considering calculation approaches, rebar layout, and meeting standard requirements. The rebar layout, steel percentage, and other parameters vary for different elements, limiting their potential uses. This study focuses on the use of manufacturing robots to expand the possibilities of these elements. The robots can modify the elements by attaching steel connections or cutting and milling techniques. In this article, the objective is to develop a technique adaptable to concrete elements, and robots were used to attach three types of joints to beams, showcasing the capabilities of robotic manufacturing. A 70-year-old building's floor slab was selected to fabricate the beam elements to demonstrate the repurposing potential. The robot-assisted manufacturing process occurred at the Digital Building Laboratory (DBFL) of the Institute of Structural Engineering (ITE) at the Braunschweig University of Technology, which houses two robot arms with

different axes and free coupling. Since the exact dimensions of the original floor segments ($30 \times 45 \times 250$ cm) in this study did not correspond to those of the selected test specimen ($10 \times 10 \times 50$ cm), these had to be cut precisely to obtain cross-sections of 10×10 cm.

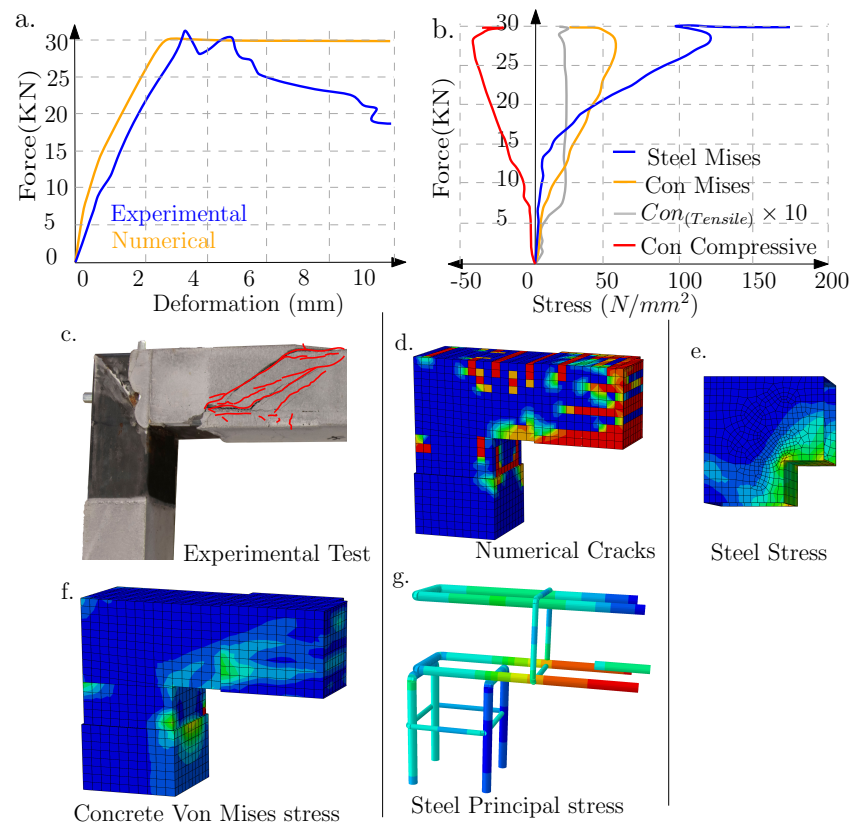


Figure 12. C5, (a) experimental and numerical force-deformation, (b) numerical tensile and compressive stress in the steel and concrete, (c) experimental cracks, (d) numerical cracks, (e) L-tube Von Mises stress, (f) concrete Von Mises stress, and (g) principal stress of rebars.

The cutting process was controlled in DBFL while vacuum supports were used to fasten the floor elements Figure 13. The cutting was performed in the DBFL with a CNC saw (Blade 5 from the company OMAG Spa, Zanica, Italy). Three different subtractive processes were performed after fabricating the beams with 10×10 cm sections. The clamping system was modified for this process, then CNC techniques were used to implement the G-codes, including drilling, sawing, and milling. The geometries of the table and clamping tools, along with the details of the joints, were modelled as CAD files, imported into the CNC software (EasyStone6.8d1). (EasyStone), and synchronised with the robot to avoid collisions.

After measuring the workpieces with 3D probes in the workspace, they were automatically machined using a G-code previously created in CAM software with the help of selected drilling and grinding tools, Figure 14. CNC technology allowed precise and repeatable results compared to manual machining. Finally, the steel tubes, hinges, and couplings were attached to the joints with and without adhesive. The ability of the robotics to process the reused elements is demonstrated in Figure 15.

Coupling Bolts: When attaching the coupling joint, two tasks are required: cutting space for the couplings and drilling holes for the screws. The robot used a saw and drill, employing two different coupling setups to ensure unrestricted access and prevent collisions. Some important points to consider about this process are as follows: (1) Cutting and drilling concrete can be expensive. (2) Placing bolts or glueing rebar at the corners of sections, crucial for proper connection between concrete and steel, can lead to unforeseen damage if stirrups are missing, Figure 15. (3) Reused elements need careful evaluation

to determine the location of internal reinforcing bars. This can be done by referring to calculation documents of the original structure or by scanning the elements. (4) Locating the rebars (using scans or original construction documents) is crucial to ensure that holes are not drilled at these locations.



Figure 13. Re-utilisation of the concrete floor elements as the beams.



Figure 14. Robotic preparation for the attachment of the three types of joints.



Figure 15. Attaching the joints to the re-utilised elements, (Left) coupling connection (C1), (Middle) steel tube connection (C4) (Right) hinge connection (C2).

Hinges: The hinges can be attached to the concrete using a robot drill to create holes at any desired angle. The angles relative to the coupling joints facilitate the process and decrease the likelihood of concrete damage. As mentioned in the performance evaluation, the angles play a crucial role in the strength of the joints. The robot can simply create the required holes at a wide range of angles. This process was performed in one setup and with G-codes for both sides of the beam (Figure 13).

Steel-Tubes: Two techniques for locating steel are robotic sawing and milling. Sawing is faster for simple geometries but can be affected by vibrations. Milling increases accuracy but also increases cost and manufacturing duration. Precision is important for joint capacity, especially if a gap exists between concrete sides. Precise milling increases friction between steel and concrete. Possible solutions are press fits or a larger gap for adhesive or mortar injection (Figure 13).

2.3. Proposed Geometries for Assemblies of Foldable Precast Elements and Their Advantages

After presenting the possible joints and the robotic operations, this section (Figures 16–20) illustrates the collected ideas for making the final geometries of the precast buildings. As

shown, the proposed geometries begin with simple floors and beams and progressively expand to multi-story buildings. All the proposed structures were created by the previously discussed connections.

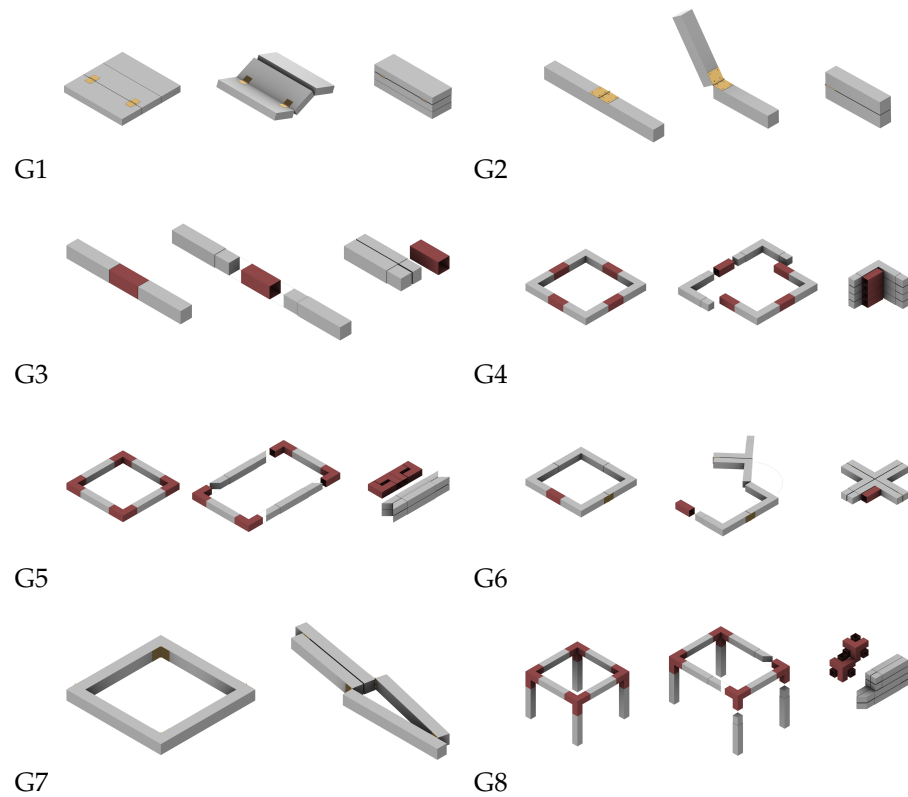


Figure 16. Proposed geometries for assemblies of foldable precast elements and structures (G1–G8).

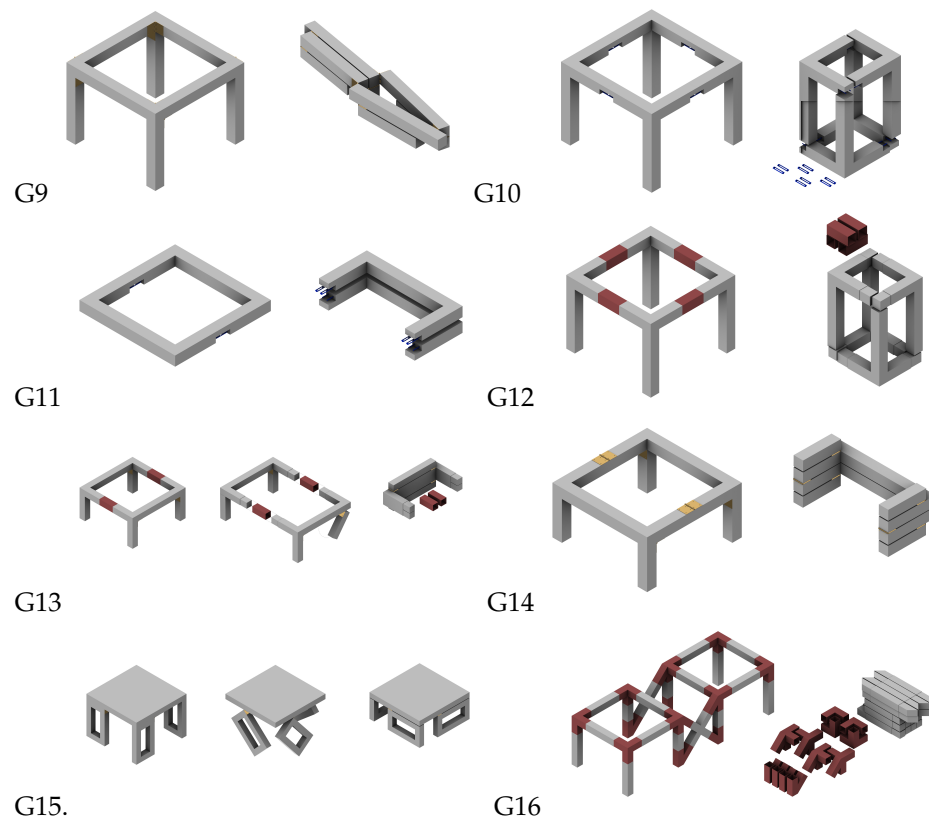


Figure 17. Proposed geometries for assemblies of foldable precast elements and structures (G9–G16).

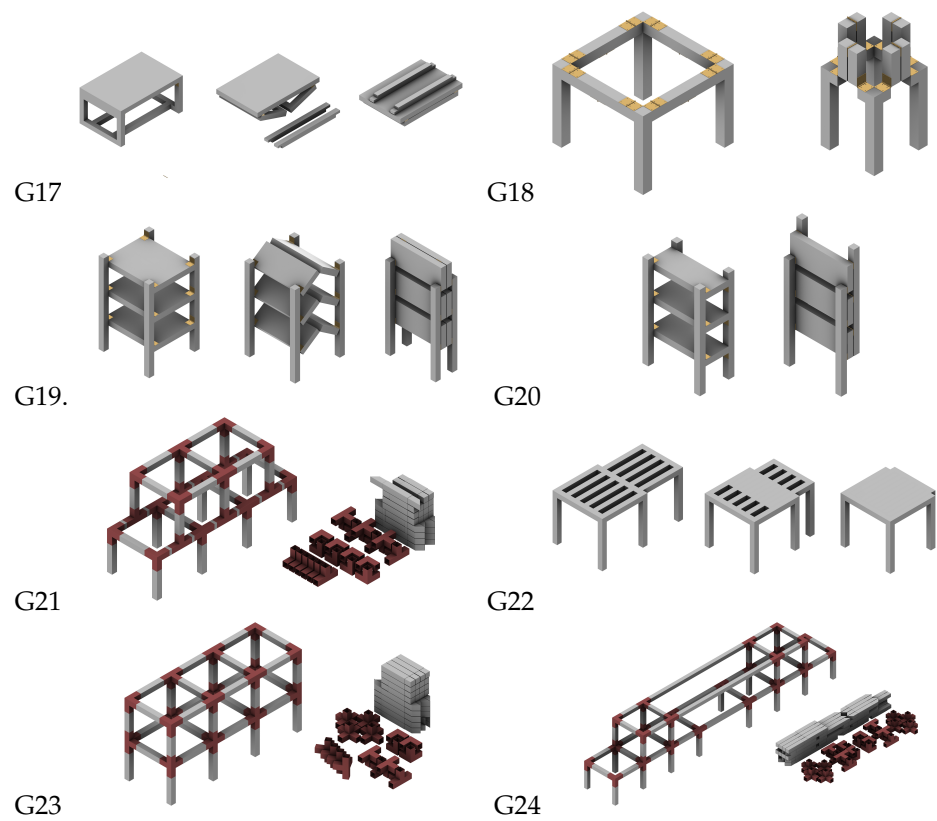


Figure 18. Proposed geometries for assemblies of foldable precast elements and structures (G17–G24).

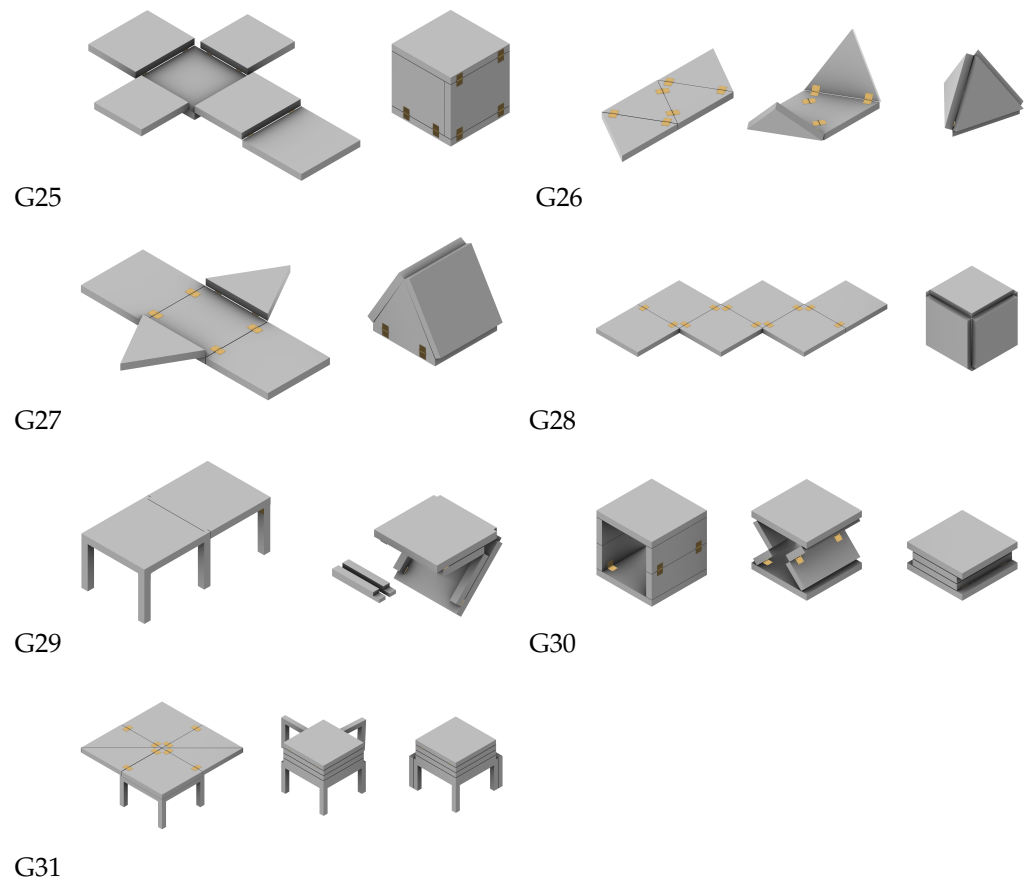


Figure 19. Proposed geometries for assemblies of foldable precast elements and structures (G25–G31).

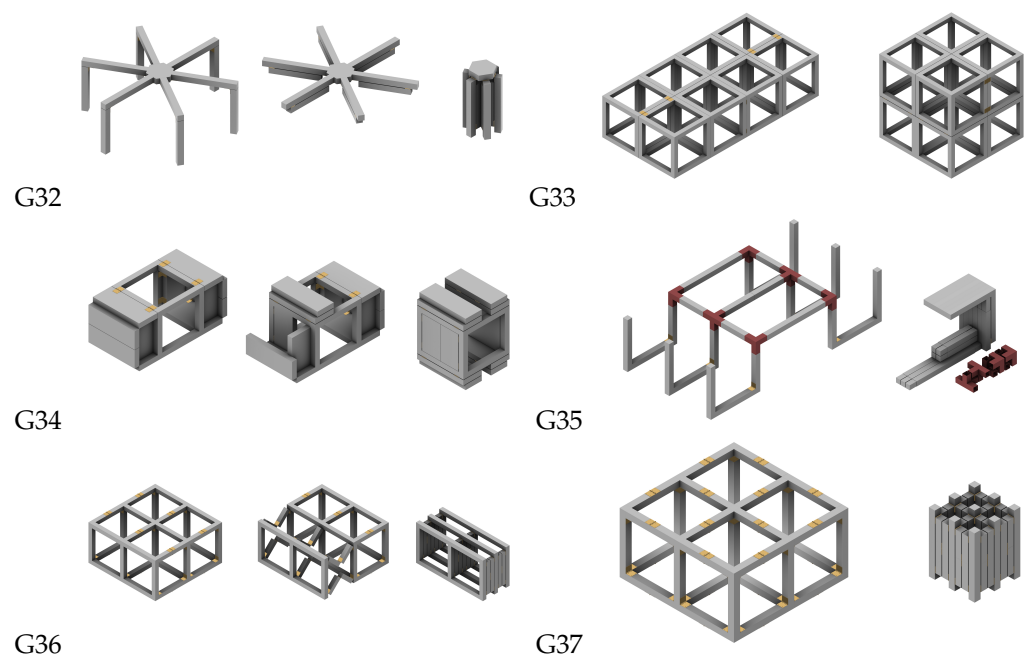


Figure 20. Proposed geometries for assemblies of foldable precast elements and structures (G32–G37).

There are several advantages to using pre-assembled and foldable concrete structures in construction compared to producing poured concrete structures on site. (1) Time savings: They can be produced in a controlled environment and installed directly on-site. This significantly reduces construction time as no time is needed for pouring and curing the concrete on site. (2) Cost efficiency: Labour costs can be reduced as less manpower is required on site. Material costs can also be reduced as the concrete can be produced more efficiently and accurately in a factory environment. (3) Quality control: They are produced under strict quality control standards and manufactured in a controlled environment. This ensures a higher quality and consistency of concrete, resulting in more durable and stable structures. (4) Flexibility and reusability: They offer high flexibility as they can be easily disassembled and reused elsewhere. This enables efficient use of resources and waste reduction. However, it is important to note that using pre-assembled, foldable concrete structures is not suitable for all construction projects. The decision to use this technology should be made based on a thorough analysis of the specific requirements and conditions of the project.

Comparison of the Proposed Foldable Geometries

This section proposes 37 geometries from unspecified structures that can be created through adjustments or combinations of the proposed re-utilised elements. In addition, designers can develop various other geometries using the proposed connections. The proposed geometries begin with the simplest and gradually become larger and more complex. The most straightforward geometry consists of two concrete elements Figure 16 (2), and the largest was designed with 57 elements Figure 20 (37). On average, they contain approximately 12 elements. Since these geometries are proposed conceptually, their dimensions are not explicitly defined. Nevertheless, to be compared with the experimental and numerical studies (previous sections), their assumed section is 10×10 cm, and the length of the beams is 1 m (called *Scale* = 1). These dimensions were assumed to be compatible with previous research and easy to scale up. For example, if the dimensions are tripled, the sections will be 30×30 cm and the length 3 m, which can be used in typical constructions. All geometries proposed above can be scaled up. The relationship between the demotions in different geometries should be the same. This means that all geometries can be, for example, scaled up 3 or 4 times in 3D (x, y, z), with the majority of

them also able to be scaled up in 2D. It enlarges perpendicular dimensions by two separate amounts, for instance, four times larger in the x-direction and three times larger in the y- and z-direction (height).

The basic dimensions of the elements are listed in Tables 1 and 2. The dimensions are illustrative and can be scaled according to various factors. In addition to scaling, some elements can also be extended. A longer beam with more spans was chosen in G24 to demonstrate the possibility of using different beam lengths. When designing the elements, an attempt was made to achieve the most compact folding layout relevant for transportation, taking into account the limitations of the hinges during the folding process. Another main factor can be the difference from the initial elements' dimensions (x, y, z). In other words, not only should the dimensions of each transport parcel be limited, but if transport by semi-trailer truck is considered, the width in two dimensions should preferably be similar (e.g., less than 3 m) and follow the traffic rules.

Table 1. Folded dimensions geometries.

Name	G1	G2	G3	G4	G5	G6	G7	G8	G9	G10	G11	G12	G13	G14	G15	G16
H (m)	0.31	0.21	0.1	0.4	0.2	0.1	0.1	0.4	0.21	0.5	0.5	0.504	1	0.43	0.51	0.4
W (m)	0.34	0.1	0.18	0.3	0.996	1.009	0.468	0.2	0.468	0.85	0.1	0.845	0.42	1	1.1	0.508
L (m)	1	0.5	0.5	0.5	0.2	1.01	1.872	0.996	1.872	0.6	1	0.6	0.5	0.5	1.1	0.996
Name	G17	G18	G19	G20	G21	G22	G23	G24	G25	G26	G27	G28	G29	G30	G31	G32
H (m)	1	1.07	1.94	2.1	0.8	1.1	0.9	3.496	1	0.985	1.021	1.209	1	0.43	1.08	1.001
W (m)	0.414	0.59	0.43	0.32	0.4	1.1	0.4	0.4	1	1.011	1.157	1.209	0.43	1	1.16	1.21
L (m)	0.5	0.59	1	1.3	0.996	1	0.996	0.5	1	1.172	1	1.209	1	1	1.16	1.21
Name	G33	G34	G35	G36	G37											
H (m)	2	1.34	1.099	1.9	1											
W (m)	2	1	0.6	0.76	0.76											
L (m)	2.01	1	1.81	1	0.76											

Table 2. Opened dimensions geometries.

Name	G1	G2	G3	G4	G5	G6	G7	G8	G9	G10	G11	G12	G13	G14	G15	G16
H (m)	0.1	0.1	0.1	0.1	0.1	0.1	0.1	0.75	0.75	0.75	0.1	0.75	0.5	0.5	0.8	0.75
W (m)	1	0.1	0.1	1	1	1	1	1	1	1	1	1	1	1	1	2.609
L (m)	1	1	1	1	1	1	1	1	1	1	1	1	1	1	1	1
Name	G17	G18	G19	G20	G21	G22	G23	G24	G25	G26	G27	G28	G29	G30	G31	G32
H (m)	0.75	0.75	1.6	1.6	1.5	1	1.5	1.5	0.21	0.1	0.25	0.1	0.75	1	0.75	0.9
W (m)	1.5	1	1	0.6	2.8	1.9	2.8	7.1	2.6	2.5	2.744	4	2	1	2	2.374
L (m)	1	1	1	1	1	1.1	1	1	3.61	0.866	3.001	3	1	1	2	2.106
Name	G33	G34	G35	G36	G37											
H (m)	1	0.9	1	1	1											
W (m)	4	2	3.8	2	2											
L (m)	2	1	1.948	2	2											

Volume Compression: The following compressions were reached based on the assumed basic dimensions (section: 10 × 10 cm and length: 1 m). The geometries result in different volumes, and the volumetric amounts were compared in three different ways: (1) the initially folded geometry (carrying size), (2) the volume after opening (final struc-

tures), and (3) the volume of all elements per geometry (concrete amounts). Table 3 shows the volumetric amounts for comparison. The compression of the final geometries (*Scale* = 1) showed a wide range of amounts, ranging from 0.01 m³ (G2) to 0.8 m³ (G33). This is equivalent to 0.024 and 1.92 tons. The average volume of concrete is 0.215 m³.

Table 3. Comparing the volumes.

Name	G1	G2	G3	G4	G5	G6	G7	G8	G9	G10	G11	G12	G13	G14	G15
height (m)	0.31	0.21	0.10	0.40	0.20	0.10	0.10	0.40	0.21	0.50	0.50	0.50	1.00	0.43	0.51
width(m)	0.34	0.10	0.18	0.30	1.00	1.01	0.47	0.20	0.47	0.85	0.10	0.85	0.42	1.00	1.10
length(m)	1.00	0.50	0.50	0.50	0.20	1.01	1.87	1.00	1.87	0.60	1.00	0.60	0.50	0.50	1.10
Opened To folded	0.95	0.95	1.11	1.67	2.51	0.98	1.14	9.41	4.08	2.94	2.00	2.94	2.38	2.33	1.30
Open to Concrete	1.00	1.00	1.02	2.84	2.88	2.79	2.78	12.64	12.06	12.68	2.90	12.22	9.69	9.62	4.15
Name	G16	G17	G18	G19	G20	G21	G22	G23	G24	G25	G26	G27	G28	G29	G30
height (m)	0.40	1.00	1.07	1.94	2.10	0.80	1.10	0.90	3.50	1.00	0.99	1.02	1.21	1.00	0.43
width(m)	0.51	0.41	0.59	0.43	0.32	0.40	1.10	0.40	0.40	1.00	1.01	1.16	1.21	0.43	1.00
length(m)	1.00	0.50	0.59	1.00	1.30	1.00	1.00	1.00	0.50	1.00	1.17	1.00	1.21	1.00	1.00
Opened To folded	9.67	5.43	2.01	1.92	1.10	13.18	1.73	11.71	15.23	1.97	5.2	1.74	1.47	3.49	2.33
Open to Concrete	13.28	4.81	12.10	5.26	5.22	18.17	11.48	15.49	21.81	4.04	1.25	5.33	2.00	6.28	2.78
Name	G31	G32	G33	G34	G35	G36	G37								
height (m)	1.08	1.00	2.00	1.34	1.10	1.90	1.00								
width(m)	1.16	1.21	2.00	1.00	0.60	0.76	0.76								
length(m)	1.16	1.21	2.01	1.00	1.81	1.00	0.76								
Opened To folded	2.06	3.07	1.00	1.34	6.20	2.77	6.93								
Open to Concrete	6.12	37.48	9.62	3.52	29.38	14.18	14.18								

The first models, (G1–G7), and G11 are the two-dimensional elements representing the base geometries of the beams, walls, and portal frames. These geometries cannot be used independently, only as a part of the structures. Therefore, these geometries cannot be compared to those with combined frames and floors (buildings). Consequently, these geometries do not have a high expansion ratio. The concrete volume and opened elements volume ratio in G1–G3 is around 1, compared to 2.8 in G4–G7. They are small components of complete structures, but they are mentioned here to emphasise the significance of the columns and folding system in achieving a high ratio of open-to-folded geometry dimensions, as opposed to two-dimensional elements, which could be floor elements.

With G8, columns were gradually added to the geometries, and one-storey structures with one floor were designed. The average amount of elements used in them is 9.1, while the maximum number can be found in G16 with 20 elements, representing a robust three-span building. G15–G17 use the largest volume of concrete, while the rest average around 0.058 m³. Considering the ratio of open-to-folded volume, it can be seen that G8 and G16 show the most optimal behaviour, while G15 has the least. G15 also has the lowest ratio of opened-up volume to concrete volume, indicating the low efficiency of these models with one floor and columns.

G21, G23, and G24 use the steel tube connection, which was investigated experimentally and numerically for two separate shapes. These geometries demonstrate that this type of joint can accommodate more branches with varying angles (e.g., cross beams, columns, and bracers). This type of connection and these three geometries are robust and can be extended indefinitely in size and height, for example by four or five storeys. Comparing the opened geometries with folded elements reveals that G21, G23, and G24 can expand up to

13.3, 11.7, and 15.23 times, respectively. As mentioned and shown in G24, these connections facilitate the expansion of beams or columns.

Generally, geometries with planar elements, such as G25–G31, showed comparable performances. Like origami geometries, these geometries could not increase the opened-to-pure concrete ratio to more than 6.2. This is due to the presence of the large solid elements. However, the paper discusses an initial general concept that must be adjusted. For example, the side walls of these models are assumed to have no openings. However, the walls can be replaced with portal frames or large windows. Additionally, basic geometries such as G4 or G5 can replace the side walls. Such modifications can significantly reduce the volume of concrete and increase the ratio.

As shown in Table 2, G24 has the largest dimension of the opened-up geometries, followed by G33 and G35. However, these geometries represent different elements, such as a beam, a floor, or an entire structure and, therefore, should be discussed separately. Since one of the primary goals of discussing foldable geometries is to highlight the different space requirements of folded-up and opened geometries, comparing the changes in dimensions is essential. For example, G33 has one of the largest dimensions, can create a sturdy structure with simple assembly, and has a high expansion compared to the amount of concrete (pure “Opened to Concrete”), whereas the differences between the folded and opened geometries (structures) are minimal. This known geometry does not demonstrate a low transportation volume, but as mentioned, due to the traffic transportation rules, such a separation of the structure to cubic elements eases transportation. As the largest opened-up volume, G24 is not only capable of multi-floor construction and has an adaptable geometry, but it can also significantly expand its dimensions (15 times). G21 shares similar characteristics. Compared to the initial material, G32 and G35 have the greatest expansion after opening (37.5 and 29.4 times larger).

The proposed geometries can be used in combination. For instance, elements like (G1, G2) and (G25–G28) can be ceiling components for the frame-shaped elements like (G16, G18, G21–G24, G32–G37). In some models, the gravity load might be in the direction of closing the structure. It means the structure does not stay in the opened-up position (final structure geometry) and partially folds back to its closed position. For instance, under their weight, the top beams in model G36 might be folded (unstable). Generally, in an optimal structure, the weight should aid in increasing the structure’s stability and maintaining its final geometry. Several solutions for this issue can be considered: (1) Changing the direction of the hinges. For instance, for the top beams in G36, the direct solution is putting the hinges on the bottom side of the beam sections. However, this causes the initial model (folded element) to be larger and transportation to be more challenging. (2) The solution to moderate the issue is locating two hinges in the beam, with lower bending (e.g., 1/3 of the beam span). (3) Using other types of connections in this zone. For instance, the top beams of G36 can be constructed without hinges using steel tubes or coupling joints. The connections can be added in the last step when the structure is opened-up. (4) A solution that can be generally used in different elements and connecting zones is the post-tensioning technique. This technique is adaptable to different geometries, resolves the difficulties mentioned above, and considerably improves the elements’ capacity (e.g., beams, columns and connections).

3. Conclusions

The study aimed to discuss a semi-new school of thought about the structure of precast concrete elements. The research regards three main points new in the precast concrete industry: firstly, using new types of connections, then re-utilising the concrete elements, and finally, the possibility of developing new geometries (such as foldable geometries) for the precast structures. This article suggests using three different types of connections as primary components. During the five experimental and numerical analyses, the performance of these connections was discussed. Their respective performances were compared to monolithic elements with the exact dimensions. The steel tubes demonstrated

a robust performance reaching up to 86% of the monolithic beam's performance, but the hinge connections only reached 24%. As previously discussed, the weak performance of the hinges resulted from the low quality of the hinges used. They were chosen because the study is primarily conceptual and introduces connections and geometries. This means that their capacity can be significantly increased. Hinges and steel tubes were studied head-to-head and head-to-side, demonstrating their adaptability to different geometrical details.

In the next section, the study illustrated the possibility of using automated manufacturing techniques using robots to prepare the connections of concrete specimens. Since the possibility of reusing old concrete elements from demolished structures was discussed, the attachment was examined, while old floor elements were selected to be reused as the beams. It was demonstrated that robotic milling, sawing, and drilling could manage all three types of connections. The final section proposed various geometries that the discussed joints could create. These geometries were developed to facilitate transportation and speed up assembly through foldable elements. Thus, 37 geometries ranging from simple floors and beams to multi-storey buildings were discussed and properties such as their volume were compared. It was discovered that some folded geometries could have around 7% of the opened-up structures (in the basic model ($Scale = 1$)). The difficulties of using these geometries, like reducing the capacity of sections by locating the hinges in non-optimal structural positions, were discussed. Furthermore, solutions, like post-tensioning techniques, were suggested to face these issues. As an initial step, this study proved the possibility of using more innovative ideas to design the joints and geometries, along with the ability of the robots. Nonetheless, it demands further steps for practical usage, including enhancements and more evaluation of the connections and standard designs of buildings by these types of joints and geometries.

The five connected elements were compared to the monolithic elements with exact dimensions as the beam and portal frame reference. Connection 3, as the weakest joint, resists up to 38% of the monolithic element while the tube connection in the same geometry with low post-tensioning force and thick tube thickness covers 86%. Similarly, the portal framed connected by hinges has a lower capacity equal to 76% of the monolithic beam, while the L-shape connector's capacity is even slightly higher than the monolithic frame.

In addition to collecting the dimensions of the design geometry, two main criteria were calculated to compare the advantages of the proposed geometries. The "Opened-To-Folded" criterion, which assesses the volume of folded elements for transport relative to the final construction, indicates that, in terms of size, the most manageable transportation would be experienced by G.24, which is 15.23 times smaller than the final construction. Among all structures (excluding individual elements like G_1 , G_2 , and G_3), G.33 has the lowest value at 1. On average, the designed structures are 3.74 times smaller during transportation. Meanwhile, the average ratio of opened dimensions to the required elements (concrete) volume is 9.03 times larger. In this case, the most efficient design is G.32, which is 37.48 times larger than the required elements.

Author Contributions: Conceptualization, A.B. and H.K.; Methodology, A.B. and L.L.; Formal analysis, A.B.; Resources, L.L.; Data curation, L.L.; Writing—original draft, A.B.; Writing—review & editing, H.K.; Supervision, H.K.; editing H.K.; validation, A.B. and L.L.; visualization, A.B. and L.L. All authors have read and agreed to the published version of the manuscript.

Funding: In a cooperation of two projects The research in this paper was developed within the research project Fertigteile 2.0 (Precast Concrete Components 2.0), funded by the Federal Ministry of Education and Research Germany (BMBF) through the funding measure "Resource-efficient circular economy-Building and mineral cycles" (ReMin) and was conducted within the scope of "Principles for Combination of Concrete Elements Produced by Different Additive Manufacturing Processes (C05)", project within the collaborative research center "Additive Manufacturing in Construction: The Challenge of Large Scale", funded by the Deutsche Forschungsgemeinschaft (DFG, German Research Foundation). Publication was supported by the Open Access Publishing at TU Braunschweig.

Data Availability Statement: The data presented in this study are available on request from the corresponding author.

Conflicts of Interest: The authors declare no conflicts of interest.

References

- European Commission. *DIRECTIVE 2008/98/EC of the European Parliament and of the Council of 19 November 2008 on Waste and Repealing Specific Directives (Text with EEA Relevance)*; European Commission: Brussels, Belgium, 2008.
- EU. Regulation (EU) No 305/2011 of the European Parliament and of the Council of 9 March 2011. *Off. J. Eur. Communities* **2016**, *269*, 1–15.
- Fiol, F.; Thomas, C.; Manso, J.M.; López, I. Transport mechanisms as indicators of the durability of precast recycled concrete. *Constr. Build. Mater.* **2021**, *269*, 121263. [[CrossRef](#)]
- Liu, D.; Li, X.; Chen, J.; Jin, R. Real-time optimization of precast concrete component transportation and storage. *Adv. Civ. Eng.* **2020**, *2020*, 5714910. [[CrossRef](#)]
- Xu, Z.; Wang, S.; Wang, E. Integration of BIM and energy consumption modelling for manufacturing prefabricated components: A case study in China. *Adv. Civ. Eng.* **2019**, *2019*, 1609523. [[CrossRef](#)]
- Polat, G. Factors affecting the use of precast concrete systems in the United States. *J. Constr. Eng. Manag.* **2008**, *134*, 169–178. [[CrossRef](#)]
- Li, C.Z.; Hong, J.; Fan, C.; Xu, X.; Shen, G.Q. Schedule delay analysis of prefabricated housing production: A hybrid dynamic approach. *J. Clean. Prod.* **2018**, *195*, 1533–1545. [[CrossRef](#)]
- Wu, G.; Yang, R.; Li, L.; Bi, X.; Liu, B.; Li, S.; Zhou, S. Factors influencing the application of prefabricated construction in China: From perspectives of technology promotion and cleaner production. *J. Clean. Prod.* **2019**, *219*, 753–762. [[CrossRef](#)]
- Fang, Y.; Ng, S.T. Genetic algorithm for determining the construction logistics of precast components. *Eng. Constr. Archit. Manag.* **2019**, *26*, 2289–2306. [[CrossRef](#)]
- Karin, W.; Lutz, B.G.; Gunter, M.; Franz, G.S. Building Materials from Waste. *Mater. Trans.* **2003**, *44*, 1255–1258.
- Hendriks, C.F.; Jensen, G.M.T. Application of construction and demolition waste. *Heron* **2001**, *46*, 95–108.
- Rathmann, K. *Recycling and Reuse of Building Materials*; National Pollution Prevention Center for Higher Education: Ann Arbor, MI, USA, 1997.
- Yadhu, G.; Devi, S.A. An innovative study on reuse of demolished concrete waste. *J. Civ. Environ. Eng.* **2015**, *5*, 1.
- Brütting, J.V.; Ervaeren, C.; Senatore, G.; De Temmerman, N.; Fivet, C. Environmental impact minimization of reticular structures made of reused and new elements through Life Cycle Assessment and Mixed-Integer Linear Programming. *Energy Build.* **2020**, *215*, 109827. [[CrossRef](#)]
- Lee, H.J.; Heuer, C.; Brell-Cokcan, S. Concept of a Robot-Assisted On-Site Deconstruction Approach for Reusing Concrete Walls. In Proceedings of the 39th International Symposium on Automation and Robotics in Construction, Bogota, Colombia, 13–15 July 2022. [[CrossRef](#)]
- Pan, W.; Gibb, A.G.; Dainty, A.R. Strategies for integrating the use of off-site production technologies in house building. *J. Constr. Eng. Manag.* **2012**, *138*, 1331–1340. [[CrossRef](#)]
- Arashpour, M.; Arashpour, M. Analysis of workflow variability and its impacts on productivity and performance in construction of multistory buildings. *J. Manag. Eng.* **2015**, *31*, 04015006. [[CrossRef](#)]
- Arashpour, M.; Wakefield, R.; Abbasi, B.; Lee, E.W.M.; Minas, J. Off-site construction optimization: Sequencing multiple job classes with time constraints. *Autom. Constr.* **2016**, *71*, 262–270. [[CrossRef](#)]
- Lim, S.; Buswell, R.A.; Le, T.T.; Austin, S.A.; Gibb, A.G.F.; Thorpe, T. Developments in construction-scale additive manufacturing processes. *Autom. Constr.* **2012**, *21*, 262–268. [[CrossRef](#)]
- Hwang, B.G.; Shan, M.; Looi, K.Y. Key constraints and mitigation strategies for prefabricated prefinished volumetric construction. *J. Cleaner Prod.* **2018**, *183*, 183–193. [[CrossRef](#)]
- Mao, C.; Shen, Q.; Pan, W.; Ye, K. Major barriers to off-site construction: The developer’s perspective in China. *J. Manag. Eng.* **2015**, *31*, 04014043. [[CrossRef](#)]
- Bock, T.; Linner, T. *Robotic Industrialization: Automation and Robotic Technologies for Customized Component, Module and Building Prefabrication*; Cambridge University Press: Cambridge, UK, 2015.
- Neubauer, R. Mechanisation and automation in concrete production. In *Modernisation, Mechanisation and Industrialisation of Concrete Structures*; Wiley Blackwell: Hoboken, NJ, USA, 2017; pp. 210–300.
- Pan, M.; Pan, W. Advancing formwork systems for the production of precast concrete building elements: From manual to robotic. In Proceedings of the Modular and Offsite Construction (MOC) Summit, Edmonton, AB, Canada, 29 September–1 October 2016.
- Bin Zakaria, Z.; Ali, N.M.; Haron, A.T.; Marshall-Ponting, A.; Hamid, Z.A. Exploring the adoption of Building Information Modelling (BIM) in the Malaysian construction industry: A qualitative approach. *Int. J. Res. Eng. Technol.* **2013**, *2*, 384–395.
- Papadonikolaki, E. Loosely coupled systems of innovation: Aligning BIM adoption with implementation in Dutch construction. *J. Manage. Eng.* **2018**, *34*, 05018009. [[CrossRef](#)]
- Baghdadi, A.; Ledderose, L.; Ameri, S.; Kloft, H. Experimental and numerical assessments of new concrete dry connections concerning potentials of robotic CNC manufacturing technique. *Eng. Struct.* **2023**, *280*, 115605. [[CrossRef](#)]

28. Engstroem, B. *Structural Connections for Precast Concrete Buildings*; FIB, Commission C: Lausanne, Switzerland, 2008; Volume 6. [CrossRef]
29. Khonsari, S.V.; Engl, G.L.; Parvinnia, S.M.H.; Hajialiakbari-Fini, E. Innovative structural joint tolerates high rotational and shear overload. In Proceedings of the ASME 2004 23rd International Conference on Offshore Mechanics and Arctic Engineering, Vancouver, BC, Canada, 20–25 June 2004; pp. 875–883. [CrossRef]
30. Camarena, D. Finite Element Analysis of Precast Prestressed Beam–Column Concrete Connection in Seismic Construction. Master’s Thesis, Department of Civil and Environmental Engineering Division of Structural Engineering Concrete Structures, Chalmers University of Technology, Göteborg, Sweden, 2006. Available online: <https://odr.chalmers.se/bitstream/20.500.12380/19635/1/19635.pdf> (accessed on 1 August 2023).
31. Castro, J. Seismic performance of precast concrete beam-column joints. *J. Struct. Constr. Eng. AIJ* **1994**, *455*, 113–126. [CrossRef]
32. Arciszewska-Kedzior, A.; Kunecky, J.; Hasnikova, H.; Sebera, V. Lapped scarf joint with inclined faces and wooden dowels: Experimental and numerical analysis. *Eng. Struct.* **2015**, *94*, 1–8. [CrossRef]
33. Baghdadi, A.; Heristchian, M.; Ledderose, L.; Kloft, H. Experimental and Numerical Assessments of New Concrete Dry Connections concerning Potentials of the Robotic Subtractive Manufacturing Technique. *Buildings* **2023**, *13*, 210. [CrossRef]
34. Baghdadi, A.; Heristchian, M.; Ledderose, L.; Kloft, H. Experimental and numerical assessment of new precast concrete connections under bending loads. *Eng. Struct.* **2020**, *212*, 110456. [CrossRef]
35. Hawileh, R.A.; Rahman, A.; Tabatabai, H. Non-Linear FE Transit Analysis of Pre-Cast Hybrid Beam–Column Connection. *Appl. Math. Model.* **2010**, *34*, 2562–2583. [CrossRef]
36. Kunecky, J.; Sebera, V.; Hasnikova, H.; Arciszewska-Kędzior, A.; Tippner, J.; Kloiber, M. Experimental assessment of a full-scale lap scarf timber joint accompanied by a finite element analysis and digital image correlation. *Constr. Build. Mater.* **2015**, *76*, 24–33. [CrossRef]
37. Kulkarni, S.A.; Li, B.; Yip, W.K. Finite element analysis of precast hybrid-steel concrete connections under cyclic loading. *J. Constr. Steel Res.* **2008**, *64*, 190–201. [CrossRef]
38. Porco, F.; Raffaele, D.; Uva, G. A Simplified Procedure for the Seismic Design of Hybrid Connections in Precast Concrete Structures. *Open Constr. Build. Technol. J.* **2013**, *7*, 63–73. [CrossRef]
39. Rodonò, G.; Sapienza, V.; Recca, G.; Carbone, D.C. A Novel Composite Material for foldable Building Envelopes. *Sustainability* **2019**, *11*, 4684. [CrossRef]
40. Kamrava, S.; Mousanezhad, D.; Ebrahimi, H.; Ghosh, R.; Vaziri, A. Origami-based cellular metamaterial with auxetic, bistable, and self-locking properties. *Sci. Rep.* **2017**, *7*, 46046. [CrossRef] [PubMed]
41. Kronenburg, R. *Portable Architecture: Design and Technology*; Birkhauser Verlag AG: Berlin, Germany, 2008.
42. Fox, M.; Kemp, M. *Interactive Architecture*, 1st ed.; Princeton Architectural Press: New York, NY, USA, 2009.
43. Overvelde, J.T.; De Jong, T.A.; Shevchenko, Y.; Becerra, S.A.; Whitesides, G.M.; Weaver, J.C.; Hoberman, C.; Bertoldi, K. A three-dimensional actuated origami-inspired transformable metamaterial with multiple degrees of freedom. *Nat. Commun.* **2016**, *7*, 10929. [CrossRef] [PubMed]
44. Silverberg, J.L.; Evans, A.A.; McLeod, L.; Hayward, R.C.; Hull, T.; Santangelo, C.D.; Cohen, I. Using origami design principles to fold reprogrammable mechanical metamaterials. *Science* **2014**, *345*, 647–650. [CrossRef] [PubMed]
45. Wang, Z.; Jing, L.; Yao, K.; Yang, Y.; Zheng, B.; Soukoulis, C.M.; Chen, H.; Liu, Y. Origami-Based Reconfigurable Metamaterials for Tunable Chirality. *Adv. Mater.* **2017**, *29*, 1700412. [CrossRef] [PubMed]
46. Boatti, E.; Vasios, N.; Bertoldi, K. Origami Metamaterials for Tunable Thermal Expansion. *Adv. Mater.* **2017**, *29*, 1700360. [CrossRef] [PubMed]
47. Chen, B.G.; Liu, B.; Evans, A.A.; Paulose, J.; Cohen, I.; Vitelli, V.; Santangelo, C.D. Topological Mechanics of Origami and Kirigami. *Phys. Rev. Lett.* **2016**, *116*, 135501. [CrossRef] [PubMed]
48. Yasuda, H.; Yang, J. Reentrant Origami-Based Metamaterials with Negative Poisson’s Ratio and Bistability. *Phys. Rev. Lett.* **2015**, *114*, 185502. [CrossRef] [PubMed]
49. Ding, J.; Li, B.; Chen, L.; Qin, W. A Three-Dimensional Origami Paper-Based Device for Potentiometric Biosensing. *Angew. Chem. Int. Ed.* **2016**, *55*, 13033–13037. [CrossRef]
50. Mousanezhad, D.; Kamrava, S.; Vaziri, A. Origami-based building blocks for modular construction of foldable structures. *Sci. Rep.* **2017**, *7*, 14792. [CrossRef]
51. Kuribayashi-Shigetomi, K.; Onoe, H.; Takeuchi, S. Cell origami: Self-folding of three-dimensional cell-laden microstructures driven by cell traction force. *PLoS ONE* **2012**, *7*, e51085. [CrossRef]
52. Baghdadi, A.; Heristchian, M.; Kloft, H. Connections placement optimisation approach toward new prefabricated building systems. *Eng. Struct.* **2021**, *233*, 111648. [CrossRef]
53. Baghdadi, A.; Heristchian, M.; Kloft, H. Design of prefabricated wall-floor building systems using meta-heuristic optimisation algorithms. *Autom. Constr.* **2020**, *114*, 103156. [CrossRef]
54. Rots, J.G.; De Borst, R. Analysis of concrete fracture in “direct” tension. *Int. J. Solids Struct.* **1989**, *25*, 1381–1394. [CrossRef]
55. Hillerborg, A. The theoretical basis of a method to determine the fracture energy of concrete. *Mater. Struct.* **1985**, *18*, 291–296. [CrossRef]
56. *DIN EN 1992-1-1:2011-01*; Eurocode 2: Design of Concrete Structures—Part 1-1: General Rules and Rules for Buildings. European Committee for Standardization: Brussels, Belgium, 2010.

57. Hejazi, F.; Esfahani, H.M. *Interpretive Solutions for Dynamic Structures Through ABAQUS Finite Element Packages*; CRC Press: Boca Raton, FL, USA, 2021. ISBN 9781032113517.
58. *DIN EN 1992-1-1*; Eurocode 2: Bemessung und Konstruktion von Stahlbeton- und Spannbetontragwerken—Teil 1-1: Allgemeine Bemessungsregeln und Regeln für den Hochbau. Ernst & Sohn A Wiley Company: Berlin, Germany, 2011. [[CrossRef](#)]
59. Baghdadi, A.; Kloft, H. Inspiration of Interlocking Wooden Puzzles in Swift Construction of Precast. In Proceedings of the Concrete Buildings, Fib, Conceptual Design of Structures 2021 International Fib Symposium, Attisholz-Areal, Switzerland, 16–18 September 2021. Available online: <https://www.sciencegate.app/document/10.35789/fib.proc.0055.2021.cdsymp.p066> (accessed on 1 October 2023).

Disclaimer/Publisher’s Note: The statements, opinions and data contained in all publications are solely those of the individual author(s) and contributor(s) and not of MDPI and/or the editor(s). MDPI and/or the editor(s) disclaim responsibility for any injury to people or property resulting from any ideas, methods, instructions or products referred to in the content.